processes

MDPI

*Article*

# Calculation Method of Support Load Zoning and Mechanism of Mine Pressure Behavior in Upward Mining Face across Half of the Goaf along the Panel Direction

**Yujiang Zhang [1,2], Fudong Ma [1], Guorui Feng [1,*], Shuai Zhang [1,*], Jie Li [3], Qian Wang [1], Xianfeng Zhang [1], Shule Li [1] and Yexing Chen [1]**

[1] College of Mining Engineering, Taiyuan University of Technology, Taiyuan 030024, China; zhangyujiang@tyut.edu.cn (Y.Z.); mafudong0876@link.tyut.edu.cn (F.M.); wangqian0833@link.tyut.edu.cn (Q.W.); zhangxianfeng0851@link.tyut.edu.cn (X.Z.); lishule0813@link.tyut.edu.cn (S.L.); chenyexing0789@link.tyut.edu.cn (Y.C.)
[2] Postdoctoral Centre, Shandong Energy Group Co., Ltd., Jinan 250014, China
[3] Shaanxi Yongming Coal Mine Co., Ltd., Yan'an 717300, China; ljie202401@163.com
* Correspondence: fguorui@163.com (G.F.); zhangshuai01@tyut.edu.cn (S.Z.)

**Abstract:** The 1515 mining face in Yongming Coal Mine was upward mined across half of the goaf along the panel direction. In this paper, the methods of field measurement, theoretical analysis, and numerical simulation were used to study the overlying rock fracture structure, support load characteristics, and the mechanism of mine pressure behavior across half of the goaf. The results indicate that the support load of the 1515 upward mining face across half of the goaf along the panel direction exhibits distinct zoning characteristics. The maximum support load is 1.37 times the minimum support load. The development height of the roof separation in the up-mining area is 1.74 times that in the entity coal area, at 9.1 m and 5.22 m respectively. The height of separation and hanging roof length increase and decrease, respectively, along the initial rock fracture area, tensile fracture area, structural fracture area, and compacted fracture area. Based on the definition of the variation coefficient "$m$" for immediate roof height and hanging roof coefficient "$n$", a partitioned method for calculating support loads in the upward mining face across half of the goaf was proposed. Finally, the key parameter values for support loads in each zoning were provided and validated.

**Keywords:** upward mining; across half of goaf along panel direction; mine pressure behavior; support load; zoning calculation method

check for updates

**Citation:** Zhang, Y.; Ma, F.; Feng, G.; Zhang, S.; Li, J.; Wang, Q.; Zhang, X.; Li, S.; Chen, Y. Calculation Method of Support Load Zoning and Mechanism of Mine Pressure Behavior in Upward Mining Face across Half of the Goaf along the Panel Direction. *Processes* **2024**, *12*, 680. https://doi.org/10.3390/pr12040680

Academic Editor: Adam Smoliński

Received: 26 February 2024
Revised: 27 March 2024
Accepted: 27 March 2024
Published: 28 March 2024

**Copyright:** © 2024 by the authors. Licensee MDPI, Basel, Switzerland. This article is an open access article distributed under the terms and conditions of the Creative Commons Attribution (CC BY) license (https://creativecommons.org/licenses/by/4.0/).

## 1. Introduction

The occurrence of multiple coal seams is a distinctive feature in coal deposits, and the extraction of multiple coal seams poses a common challenge in coal mining. Regarding the sequence of mining in multiple coal seams [1,2], the traditional approach primarily involves downward mining [3,4]. The opposite mining sequence is upward mining [5]. After the lower coal seam is mined and stabilized, the upper coal seam is mined. In the process of mining, the complete overlying rock strata of the lower coal is used as the upper coal floor. Upward mining finds extensive applications in protective layer mining and mitigating outburst dangers [6,7]. Nevertheless, as the lower coal seam is extracted, the overlying rock strata inevitably experience subsidence, deformation, and crack propagation, impacting the stability of the stope in the upward mining face [8,9]. Therefore, to ensure the safety of retreat mining in the upward mining face, it is crucial to study the structure of overlying strata and the calculation of hydraulic support load during upward mining.

Numerous researchers have conducted extensive research on the structure of rock strata in upward mining, yielding significant findings. Feng et al. [10–12] discovered that, in the residual mining area using the caving method, interlayer rock strata breakage in upward mining resulted in a neatly arranged and mutually squeezed "block beam-semi-arch" structure due to the shear dilation effect. Ma et al. [13] found that the extraction of the lower coal seam alters the structure of overlying rock strata and the distribution pattern of mine pressure in the upper coal seam. Zhang et al. [14] observed that when the interlayer spacing exceeds the height of the caved zone of the lower coal seam, the entire roof and floor of the upper coal seam undergo destruction, yet continuity is maintained, and over time, cracks and fractures are gradually compacted, enhancing the overall integrity of the coal seam. Through similarity simulation, Zhang [15] determined a caving angle of 65° for rock strata in the lower goaf, and identified the existence of large and small periodic pressure in the upward mining face. Kong et al. [16] obtained characteristics of roof breakage and the migration patterns of overlying rock strata in the close-range upward mining face. Wang et al. [17] proposed a "three-hinged arch" structure for the upward mining face for repeated mining of the lower roof structure. Additionally, regarding the problem of overlying strata zoning, there is a relatively consistent view among researchers worldwide about the vertical direction. Peng [18], Qian [19], and Liu et al. [20] divided the overlying rock strata into caved zone, fracture zone, and curved subsidence zone. In the horizontal direction, Qian [19] divided the front and back of the stope and overlying strata into "three horizontal zones", including the coal face support area, separation area, and recompression area. Wang [21] classified the stope-surrounding rock into initial stress area, coal face support area, separation area, recompression area, and stable area. Guo et al. [22] classified the overburden into initial rock fracture area, tensile fracture area, structural fracture area, and compacted fracture area. Many researchers working on the theoretical framework of the overlying strata structure in the mining field have studied calculation methods for the hydraulic support working resistance to achieve stable support for the mining face. Many researchers have studied the working resistance calculation method for hydraulic support under a theoretical framework system of overlying rock structure in the stope. To realize a stable hydraulic support in the mining face. Wu et al. [23] developed a mechanical model of the interaction between the support and the surrounding rock to derive a formula for calculating the hydraulic support working resistance. Li et al. [24] clarified the calculation method for hydraulic support working resistance in fully mechanized, top-coal caving mining faces in complex hard rock strata. Singh et al. [25] proposed a method to estimate the optimal bearing capacity of hydraulic support. Juárez et al. [26] presented an empirical formula for calculating the load of the hydraulic support in longwall faces. In summary, many researchers have studied extensively the structure of overlying rock strata and the manifestation of mine pressure in upward mining. However, all the studies are based on the condition that the upward mining face is entirely above the goaf. There is limited research on the movement characteristics of rocks and the manifestation features of mine pressure in the upward mining face across half of the goaf along the panel direction, where a part is above the goaf, and another part is above the entity coal. Notably, the fracture structure and stress environment of overlying rock strata above the goaf exhibit significant differences in the middle of the goaf, at the goaf boundary, and above the entity coal. Therefore, there is a need for further research into the calculation method of support load zoning and the mechanism of mine pressure behavior in the upward mining face across half of the goaf along the panel direction.

This study focuses on the 1515 upward mining face across half of the goaf along the panel direction in the Yongming Coal Mine. It employs a comprehensive method that integrates field measurements, theoretical analysis, and numerical calculations. Field measurements and analyses are conducted to assess the overlying strata fracture development of the lower coal seam, the delamination status of the roof in the upward mining face, and the loads on the hydraulic support. Based on measured data from the hydraulic support and the distinctive features of overlying strata fractures in different regions, we propose methods for calculating hydraulic support loads in three regions: up-mining area, transition area, and entity coal. The effectiveness of the proposed hydraulic support load calculation method is validated using numerical models that reveal the fracture structure of the stope and the mechanism of mine pressure zoning.

## 2. Measurement of Overlying Strata Fractures and Mine Pressure in Upward Mining across Half of the Goaf along the Panel Direction

### *2.1. Geology and Mining Conditions*

Yongming Coal Mine is located in the southwest of Zichang city in Shaanxi Province, covering an area of 9.11 km$^2$ with a longitudinal span of 3.38 km and a latitudinal span of 2.69 km, as illustrated in Figure 1a. The minefield belongs to the Upper Triassic Wayaobu Formation, and the structural form is monocline. The geology is stable within the minefield, and there are no faults, collapse columns, or magmatic intrusion. No. 5 coal seam belongs to the Class II spontaneous combustion coal seam, with a spontaneous combustion period of 52 days. Coal dust is explosive with an explosion index of 39.64%. The mine is a low-gas mine, and the maximum gas emission rate of the 1515 mining face is 0.44 m$^3$/min. The mining of the 1515 mining face is not affected by goaf water, and is less affected by surface water and groundwater, which appears in the form of roof dripping. The normal water inflow in the mining process of the 1515 mining face is about 0.5 m$^3$/h, and the maximum water inflow is 1 m$^3$/h. The primary coal seams currently exploited are No. 3 and No. 5, where No. 5 lies above No. 3 at a depth of 140–180 m. Both No. 3 and No. 5 exhibit average thicknesses of 0.7 m and 0.89 m, respectively, with a slight dip of 1° to 3°, characterizing them as nearly horizontal coal seams. The spacing between No. 5 coal seam and No. 3 coal seam is 37.6 m. Between these two coal seams, the rock types that appear from top to bottom are mudstone, siltstone, fine sandstone, and coal. The interlayer strata are 2.0 m mudstone, 6.9 m siltstone, 10.8 m fine sandstone, 2.7 m mudstone, 0.3 m coal, 3.0 m mudstone, 6.3 m siltstone, and 5.6 m mudstone. The immediate roof of the No. 5 coal seam is a 5.22 m thick gray-black mudstone, and the main roof is a 10.86 m thick siltstone. The specific details are shown in Figure 1b.

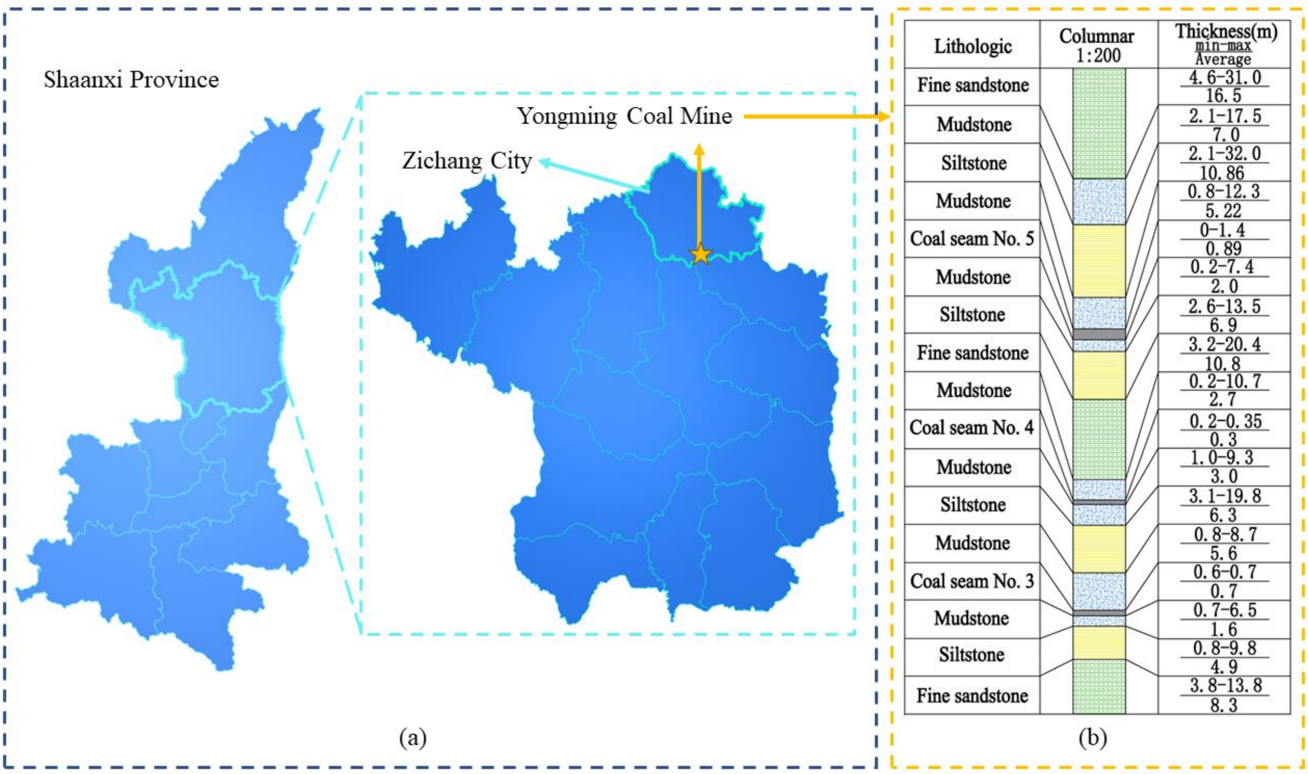


**Figure 1.** Mine location and column: (**a**) mine location; (**b**) comprehensive histogram of mining face in Yongming mine.

The 1515 mining face is situated in the No. 5 coal seam and a thin coal seam mechanized mining method with a mining height of 1.1 m is used. It extends 876 m in strike length and 200 m in dip length. The 1515 mining face is an upward mining face across half of the goaf along the panel direction, traversing both the 3105 goaf and the entity coal. Specifically, the inclined length above the goaf is 97 m, and above the entity coal, it is 103 m, as illustrated in Figures 1b and 2a.

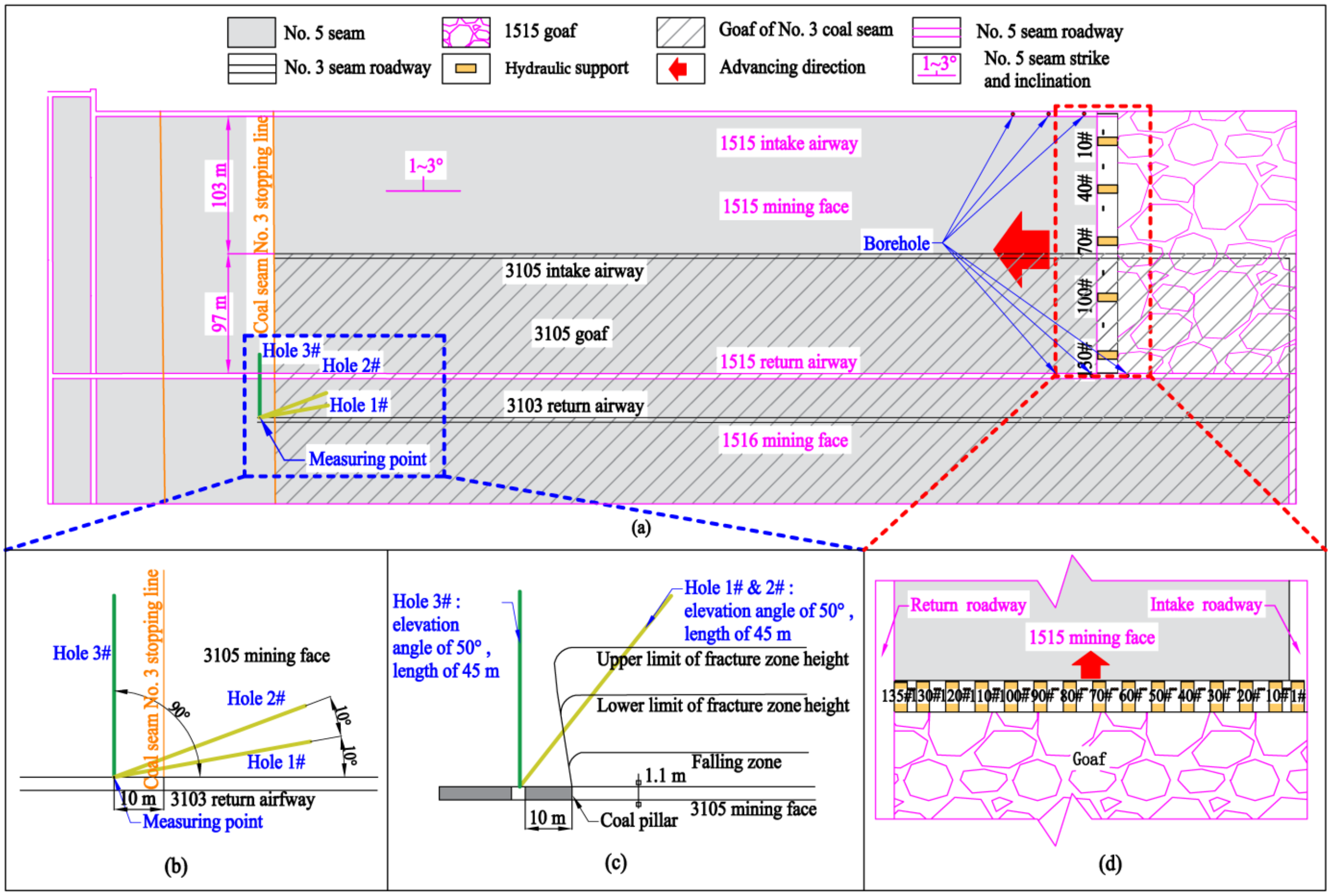


**Figure 2.** Layout of the mining face and column chart: (**a**) mining face layout; (**b**) vertical view; (**c**) roadway face sectional drawing; (**d**) mine pressure measuring point layout.

## *2.2. Upward Mining Feasibility Assessment*

Studies indicate that a prerequisite for upward mining is to extract the lower coal seam without compromising the integrity and continuity of the overlying upper coal seam [27–33]. The feasibility of upward mining in the 1515 mining face was assessed by three methods, namely, the ratio discrimination method, the rock balance discrimination method, and the discrimination method of "three zones" [34]. The formula for calculating the height of the fracture zone is given in reference [30]. The lithology has a significant influence on the development height of the "two zones", and determines the applicable calculation formula. The uniaxial compressive strength of the rock between No. 5 and No. 3 coal seams in Yongming Coal Mine is 20.7 MPa~34.3 MPa, belonging to the medium hard rock strata. Accordingly, the calculation formula in Table 1 was selected. The computed results are presented in Table 1.

The ratio discrimination method yields a mining influence coefficient of 34.7 for the 1515 mining face, significantly surpassing the threshold of 7.5. The rock balance discrimination method determines the required minimum interlayer spacing for upward mining as 17.3 m, which is less than the 37.6 m spacing between the No. 3 and No. 5 coal seams. Meanwhile, the discrimination method of "three zones" calculates a maximum fracture zone height of 30.98 m, also less than the layer spacing of the two coal seams (37.6 m). These three methods clearly indicate the feasibility of upward mining in the 1515 mining face.

**Table 1.** Feasibility calculation results for upward mining of the 1515 mining face.

| Method | Discriminant Standards | Result |
|---|---|---|
| The ratio discrimination method | The mining influence factor, $K_1 = H/M$ [29] > 7.5 [27] | $K_1$ = 34.5 > 7.5, Upward mining can be carried out. |
| The rock balance discrimination method | $H > H_p = M/(K-1) + h_p$ [27] | $H_p = 17.3$ m < 37.6 m, Upward mining can be carried out. |
| The discrimination method of "three zones" | $H > H_1 = \begin{cases} 100M/(1.6\sum M + 3.6) + 5.6 \\ 20\sqrt{M} + 10 \end{cases}$ [30] | $H_1 = 26.12$ m~30.98 m < 37.6 m, Upward mining can be carried out. |

Here, $K_1$ represents the mining influence coefficient, $H$ denotes the spacing between upper and lower coal seams (m), $M$ signifies the mining height of the lower coal seam (m), $H_p$ stands for the minimum layer spacing for coal seam mining (m), $K$ is the bulking coefficient, $h_p$ indicates the thickness of the equilibrium rock strata (m), and $H_1$ represents the height of the fracture zone (m).

### 2.3. Measurement Scheme

Upward mining across half of the goaf along the panel direction is affected by many factors. The significant factors in field measurements include the development height of "two zones" in the lower mining face, the immediate roof separation height in the upper mining face, and the load on the hydraulic supports. The significant factors are shown in Table 2.

**Table 2.** Significant measurement factors.

| Significant Factors | Description |
|---|---|
| The height of "two zones" | The feasibility of upward mining was determined by comparing the distance between coal seams calculated by contours with the theoretical height of "two zones". Furthermore, the height of "two zones" was determined by the hole seepage quantity observation method, and the correctness of the above judgment was verified. |
| The height of the immediate roof separation | By using an endoscope to check the height of the immediate roof separation, the characteristics of the overlying strata failure can be analyzed and determined. |
| The hydraulic support load | The load of the support was recorded by a pressure sensors on the support, analyzed and mine pressure behavior in the mining face obtained |

(1) Measurement scheme for development height of "two zones" in the lower mining face

The height of the "two zones" in the lower mining face was determined using the hole seepage quantity observation method. A measurement point was established 10 m away from the stopping line of the 3105 mining face, which included three drill holes. The detailed data for each hole are outlined in Table 3, and their positions are illustrated in Figure 2b,c.

**Table 3.** Elements of each hole.

| Hole Number | Azimuth Angle | Vertical Angle | Length/m | Diameter/mm | Usage |
|---|---|---|---|---|---|
| 1# | 10° | 50° | 45 | $\varphi$89 | Observation |
| 2# | 20° | 50° | 45 | $\varphi$89 | Observation |
| 3# | 90° | 50° | 45 | $\varphi$89 | Comparison |

Note: The orientation of the coordinate azimuth was taken with the opposite direction of the mining face advancement as the starting direction.

(2) Measurement scheme for the height of the immediate roof separation in the upper mining face

In this measurement, an endoscope was used to inspect the roof of mining face roadways, detecting the height of the immediate roof separation in the 1515 upward mining face. Groups of holes were strategically placed in the return airway and the intake airway of the 1515 mining face for separation height detection. Each group comprised three holes, spaced 20 m apart, with a depth of 10 m. The hole positions are depicted in Figure 2b.

(3) Monitoring scheme for hydraulic support loads in the upward mining face across half of the goaf along the panel direction

The 1515 upward mining face in Yongming Coal Mine utilized a total of 135 hydraulic supports. Fifteen of these were selected as monitoring points to record variations in support loads. These monitoring points were specifically identified as 1#, 10#, 20#, 30#, 40#, 50#, 60#, 70#, 80#, 90#, 100#, 110#, 120#, 130#, and 135#. The layout of the monitoring points for support load are presented in Figure 2d.

### 2.4. Measurement Results

(1) Height of "two zones" in the lower mining face

The water seepage quantity data recorded in each hole observation were plotted to analyze the variation of water seepage quantity in each hole. Ultimately, the height of the fracture zone in the lower mining face was determined. Figure 3 illustrates the distribution of water seepage quantity in each hole.

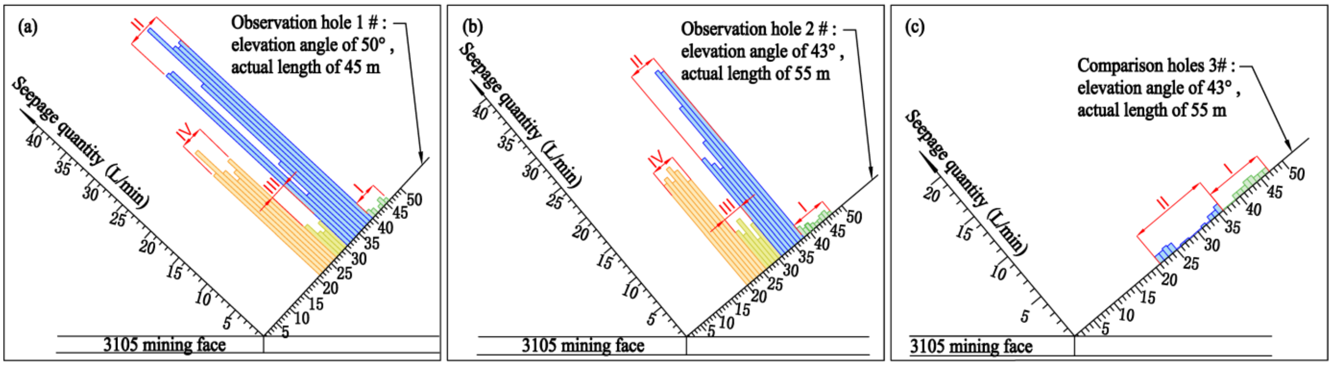


**Figure 3.** Distribution of water seepage quantity in holes: (**a**) observation hole 1#; (**b**) observation hole 2#; (**c**) comparison hole 3#.

As shown in Figure 3a,b, the II segment of observation holes 1# and 2# exhibits the maximum water seepage, with rock strata water seepage ranging from 8.3 to 38.0 L/min and 13.6 to 28.5 L/min respectively. At this point, the vertical heights are 24.12 to 29.58 m and 24.12 to 28.21 m, respectively. Consequently, the maximum observed heights of the fracture zone for observation holes 1# and 2# are determined as 29.58 m and 28.21 m. Figure 3c shows that the water seepage in the II segment of comparison hole 3# ranged from 0 to 1.0 L/min. In the II segment, the seepage water of observation holes 1# and 2# is more than that of comparison hole 3#. Therefore, the II segment of holes 1# and 2# enters the range of the fracture zone. In summary, the maximum determined height of the fracture zone is 29.58 m.

(2) Height of the immediate roof separation in the upward mining face across half of the goaf along the panel direction

The borehole inspection results are illustrated in Figure 4, revealing the development of the roof separation as follows: in the entity coal area, delamination occurs at positions 1.2 m, 3.3 m, 4.3 m, and 5.22 m above the roadway roof, with the maximum height of the immediate roof separation in the entity coal area reaching 5.22 m. In the up-mining area, delamination is observed at positions 0.9 m, 2.1 m, 4.1 m, 4.27 m, 9.0 m, and 9.1 m above the roadway roof, indicating significant development of separated fractures in the overlying strata. The maximum height of the immediate roof separation in the up-mining area is 9.1 m, surpassing the maximum height of the immediate roof separation in the entity coal area.

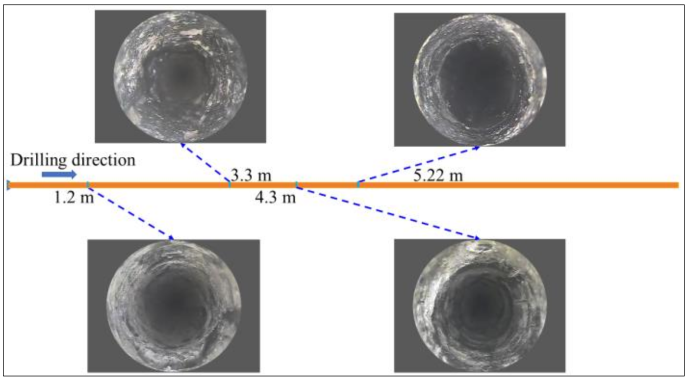


(**a**)

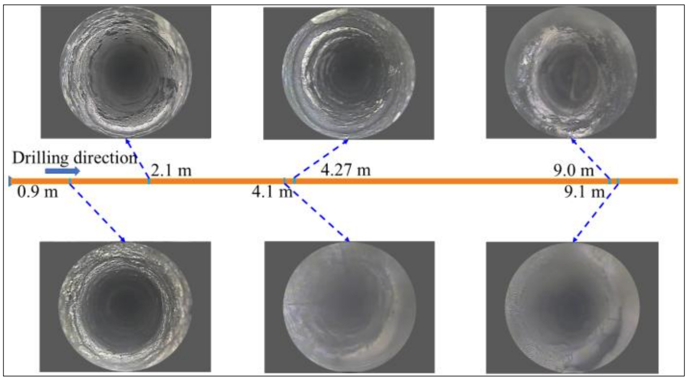


(**b**)

**Figure 4.** Hole inspection results: (**a**) the entity coal area; (**b**) the up-mining area.

(3) Analysis of the load monitoring results for hydraulic supports in the upward mining face across half of the goaf along the panel direction

Figure 5 illustrates a surface diagram showing the variation of each hydraulic support load with the mining face advancement distance. The diagram uses the mining face advancing distance, hydraulic support load, and hydraulic brace number as axes. Analyzing the characteristics of load on the mining face based on hydraulic support loads, Figure 6 illustrates the average periodic pressure step and pressure intensity of each support roof in the upward mining face.

As depicted in Figure 5, the maximum support load reaches 39.06 MPa, which is below the rated support value of 47 MPa, indicating that the strength of the supports satisfies the requirements for supporting the roof during the mining phase of the mining face. The load distributions of hydraulic supports in the 1515 upward mining face exhibit a noticeable non-uniform pattern. As the mining face advances from 0 to 90 m, both sides experience low-pressure zoning, with alternating high-pressure and low-pressure areas in the middle. As the mining face advances from 90 to 142 m, low-pressure and high-pressure areas are distributed on both sides, while the middle portion remains stable.

As shown in Figure 6a, the average periodic pressure step for each support roof exhibits minimal variation, ranging from 11.4 m to 14.8 m. As illustrated in Figure 6b, the hydraulic support loads in the 1515 upward mining face exhibit an overall pattern of alternating low and high pressure. The loads of supports 1# to 40# above the entity coal and supports 100# to 135# above the up-mining area both exhibit a distribution pattern of an initial increase followed by a decrease. Peaks are observed at supports 20# and 120#

with support loads reaching 32.8 MPa and 35.4 MPa, respectively. Although supports 50# to 90# experience slight fluctuations in load, they consistently remain in a high-load state, with support load peaking at support 60#, reaching 34.99 MPa.

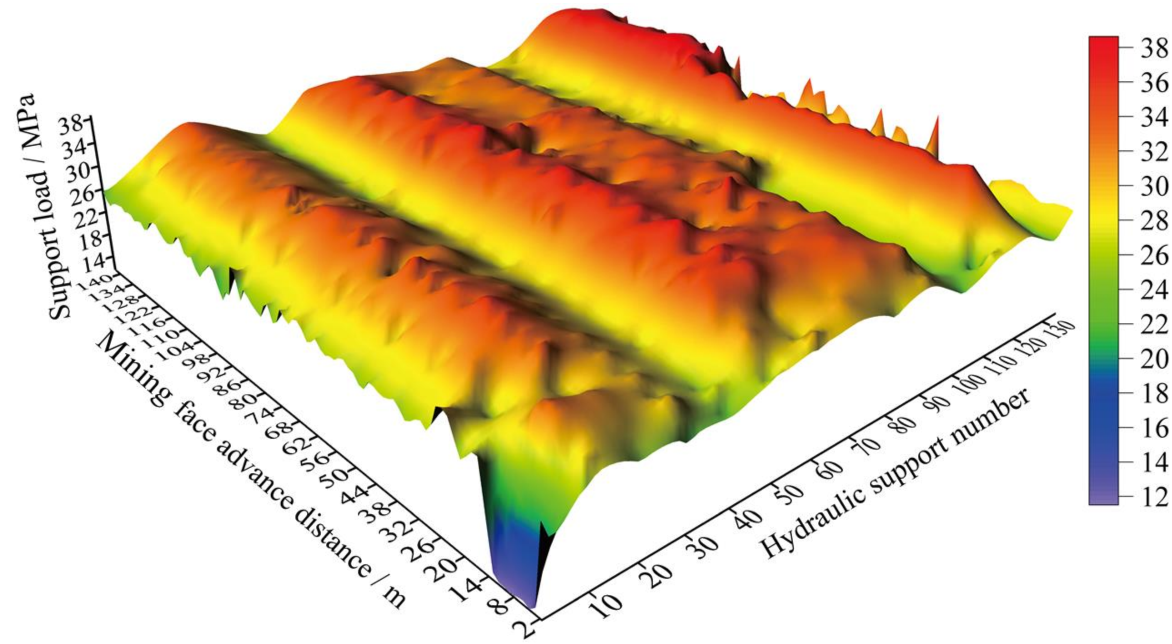


**Figure 5.** Distribution surface diagram of hydraulic support loads for the upward mining face across half of the goaf along the panel direction.

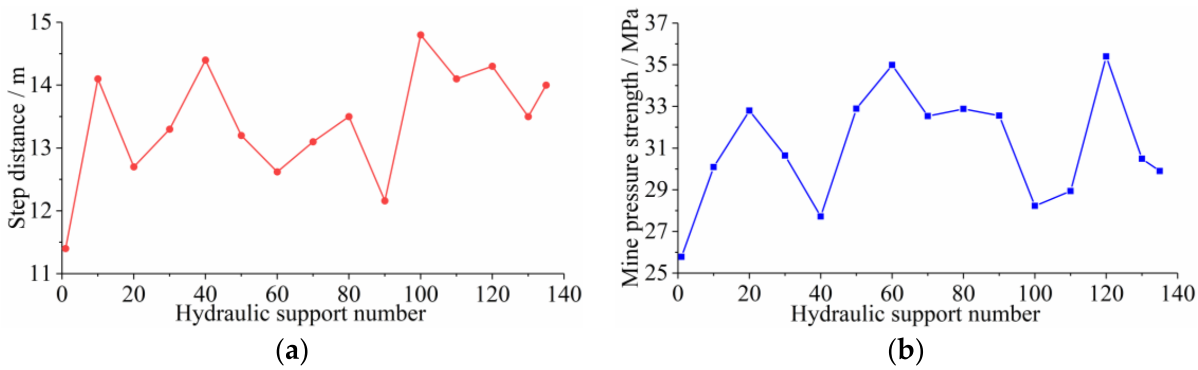


**Figure 6.** Characteristic statistics of hydraulic support pressure in the mining face: (**a**) periodic pressure step statistics; (**b**) pressure intensity statistics.

## 3. Characteristics of Mine Pressure Zoning and Support Load Calculation Methods

### *3.1. Mine Pressure Zoning Characteristics Based on Overlying Strata Fracture Structure*

Following retreat mining of the lower mining face, the portion of the rock fracture line that lies between the contour of the upper coal seam floor and the lower mining face is defined as the fracture boundary. Similarly, the portion of the line connecting the mining face to the moving basin boundary within the same area is defined as the influence boundary. The overlying strata movement fractures are divided into "horizontal four areas" based on their distribution characteristics [22], as shown in Figure 7. The initial rock fracture area is situated in the entity coal area to the right of the influence boundary, and it experiences minimal effect from the lower mining face movement, maintaining its initial rock stress state. The tensile fracture area is positioned between the influence boundary and the fracture boundary, partly above the coal pillar and partly above the goaf, forming a structure resembling a "cantilever beam". The structural fracture area is located to the left of the fracture boundary, and due to the horizontal thrust generated during the rotation process, the rock blocks formed by the main roof fracture are hinged to each other, forming a "masonry beam" structure. The compacted fracture area is located in the middle of the goaf, and with the periodic pressure of the main roof, the overlying strata separation and fractures gradually close. The specific calculation ranges are outlined in Table 4.

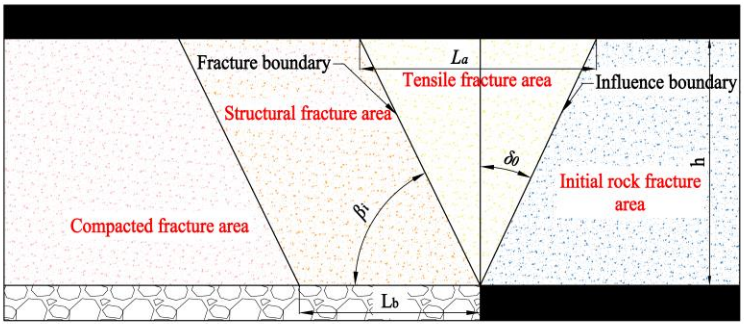


**Figure 7.** Schematic diagram of the "horizontal four areas".

**Table 4.** Overlying strata mine pressure zoning ranges in the lower mining face.

| Parameter | Formula | Result |
|---|---|---|
| Displacement angle | $\delta_0 = 27.96 - 0.02426h + 6.9 \times 10^{-6}h^2$ [18] | $\delta_0 = 24.87°$ |
| Breaking angle | $\beta_i = 45 - \varphi/2 + \left(tan^{-1}\eta\sqrt{R_T/q}\right)/2$ [22] | $\beta_i = 65.63°$ |
| Range of tensile fracture area | $L_a = H/tan\beta_i + Htan\delta_0$ [22] | $L_a = 35.09$ m |
| Range of structural fracture area | $\theta = sin^{-1}4\left[\sqrt{30(h+h_1)\rho g/\sigma_c} - tan\varphi\right]/3$ [22]<br>$L_1 = h\sqrt{R_T/3q}$ [19]<br>$L_b = [1 - (ln0.003 - ln\theta)/ln4] \times L_1$ [22] | $L_b$ = 40.15 m |

Here, in the formulas, $\delta_0$ is the displacement angle; $h$ is the overlying strata thickness, (m); $\beta_i$ is the breaking angle; $\varphi$ is the internal friction angle; $\eta$ is the strata breaking distance index; $R_T$ is the immediate roof tensile strength, (MPa); $q$ is the overlying load, (MPa); $L_a$ is the range of the tensile fracture area, (m); $\theta$ is the rotation angle of rock blocks; $h$ is the thickness of the bearing layer, (m); $h_1$ is the thickness of the bearing layer loaded by the coal seam, (m); $\rho$ is the density of the bearing layer rock, (g/cm$^3$); $\sigma_c$ is the compressive strength of the bearing layer, (MPa); and $L_b$ is the range of the structural fracture area, (m).

According to the "horizontal four areas" where the upper coal seam is located, it can be seen that there are several zones along the inclined direction of the upper coal seam mining face. In order to make the hydraulic supports reflect the load of each zone well, the support loads of 10#, 20#, 30#, 40#, 50#, 60#, 70#, 80#, 90#, 100#, 110#, 120#, and 130# are selected to draw the distribution diagram of the hydraulic supports in the "transverse four zones", as shown in Figure 8. Supports 10# to 60# are positioned in the initial rock fracture area, with an average load of 29.99 MPa. Supports 61# to 85# are located in the tensile fracture area, exhibiting an average load of 33.47 MPa. Within this area, the average support load reaches the maximum value in the "horizontal four areas" of the mining face. Supports 86# to 110# are placed in the structural fracture area, demonstrating an average load of 29.91 MPa. Within this area, the average support load reaches the minimum value in the "horizontal four areas" of the mining face. Lastly, supports 111# to 130# are positioned in the compacted fracture area, displaying an average load of 32.01 MPa. According to the results shown in Figure 4, for the immediate roof of the upper mining face, the height of the compacted fracture area is greater than that of the initial rock fracture area. Consequently, in terms of the average load of the supports, the compacted fracture area also exceeds the initial rock fracture area.

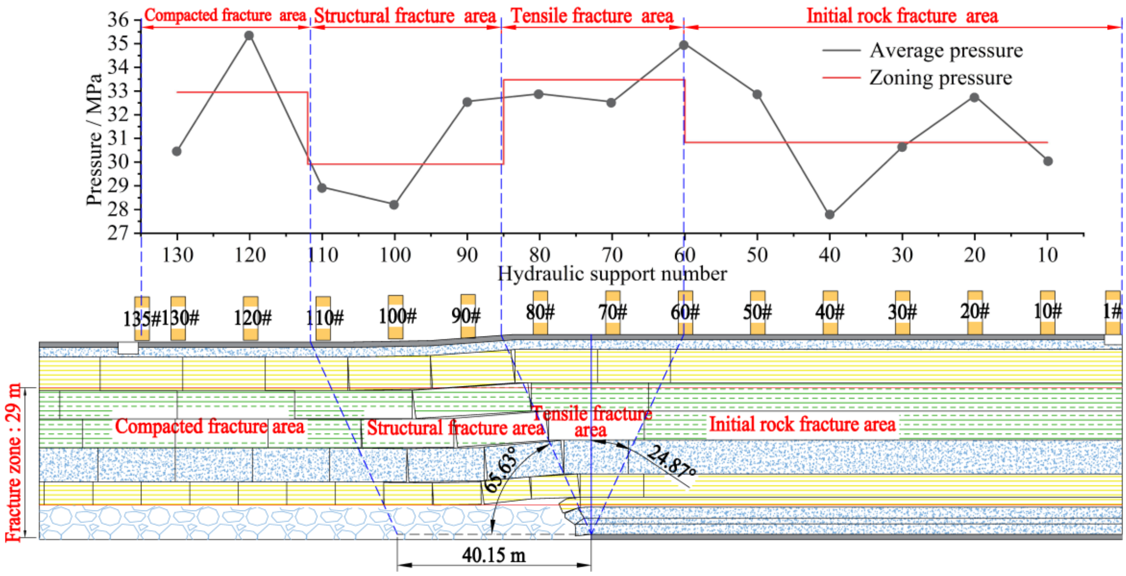


**Figure 8.** Distribution of hydraulic support loads in the "horizontal four areas".

### 3.2. *Zoning Calculation Method for Hydraulic Support Load*

Domestic and international researchers suggest that the weight of the roof can serve as the load for the support, and the load of hydraulic support can be expressed as [19]:

$$Q_i = \sum h_i L_i \gamma \tag{1}$$

where $Q_i$ is the hydraulic support load (kN/m), $\sum h_i$ is the roof separation height (m), and $\gamma$ is the volume force (kN/m$^3$). When $i$ = 1, the hydraulic support is located in the entity coal area; when $i$ = 2, it is positioned in the up-mining area.

According to Formula (1), it is evident that, for a given state of the main roof, the height of the immediate roof separation and the length of the hanging roof in different zoning directly impact the hydraulic support load. Simultaneously, the height of the roof separation and the length of the hanging roof are closely related to the fracture structure of the overlying rock in different regions. Based on these principles, the load calculation formula for hydraulic supports in different zoning can be modified. The immediate roof height variation coefficient $m$ is introduced to represent the immediate roof separation heights of different zoning. Meanwhile, the hanging roof coefficient $n$ is used to express the hanging roof length of different zoning. The modified expression of the hydraulic support load is obtained:

$$Q_1 = m \sum h_1 \mathrm{n} \mathrm{L}_1 \gamma \tag{2}$$

For non-upward mining situations, $m \cdot n$ = 1. In the case of upward mining, an analysis of parameter values for different zoning of the overlying strata fracture structure is necessary based on measured data such as the height of the immediate roof separation and the hydraulic support load. Bringing the height of the immediate roof separation (see Section 2.4 for details) of the 1515 upward mining face into the formula for calculation, where $h_1$ = 5.22 m (Figure 4a), $h_2$ = 9.1 m (Figure 4b), and $L_2 = 1.6L_1$, and $Q_1 = 8.35L_1\gamma$ and $Q_2 = 9.1L_1\gamma$ are calculated. The analysis shows that $Q_1$ is 91.2% of $Q_2$, and according to the measured data, the support load in the entity coal area is 93% of the support load in the up-mining area. It can be seen that the hanging roof length and the immediate roof height jointly determine the hydraulic support load in the 1515 mining face.

Due to the upward mining across half of the goaf along the panel direction in the 1515 mining face, it is divided into three areas: up-mining area (compacted fracture area), transition area (tensile fracture area and structural fracture area), and entity coal area (initial rock fracture area). The rock strata in the up-mining area were damaged and separated previously, and the strength of the rock strata is reduced. As a result, the length of the immediate roof became shorter and the height of the immediate roof separation became higher, as shown in Figure 9a. The rock strata in the entity coal area is less affected by No. 3 coal mining, and the rock strata structure is not prematurely destroyed. At this time, the hanging roof length is long, and the height of the immediate roof separation is low, as shown in Figure 9c. During the transition from the up-mining area to the entity coal area, the length of the hanging roof gradually increases, while the height of the immediate roof separation gradually decreases, as shown in Figure 9.

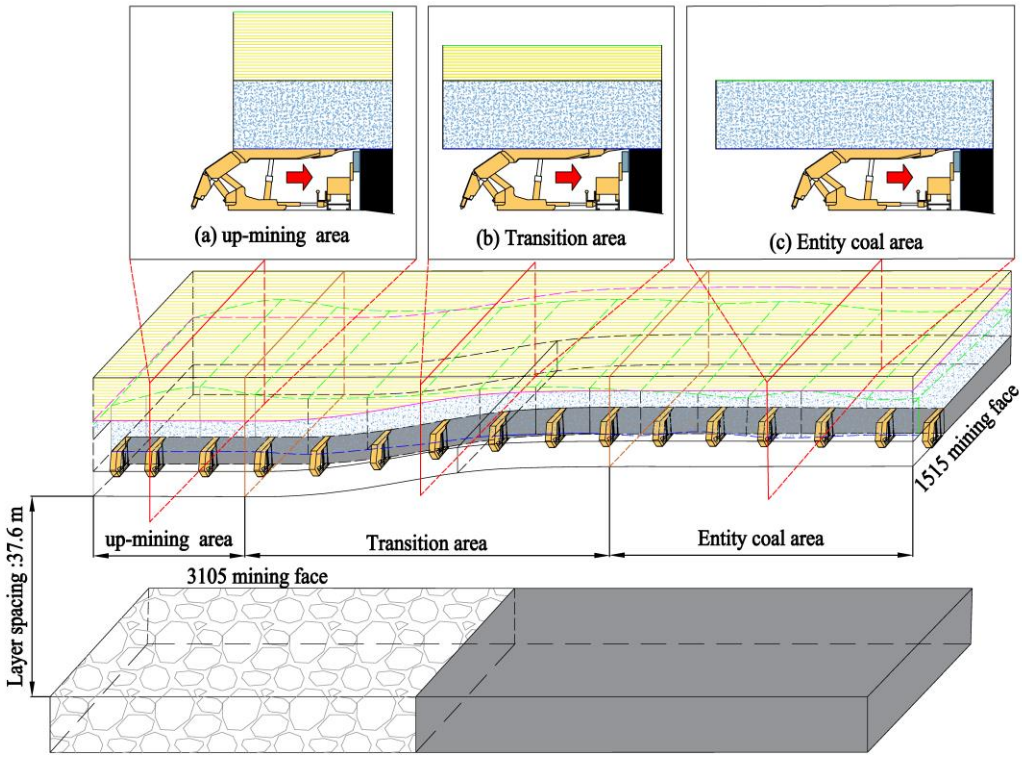


**Figure 9.** Bearing structure diagram of hydraulic support in different areas.

Based on the structural characteristics of the overlying strata in the three areas of the up-mining area, transition area, and entity coal area, the hydraulic supports' load in the entity coal area is used as a reference to study the range of support load in different areas. Formula (2) combines with the mine pressure strength for zoning calculation, can be derived separately from the hydraulic support load ranges of the three areas:

$$Q_1 = m \cdot n \sum h_1 L_1 \gamma \quad \begin{cases} m \cdot n = 1, \ \textit{Entity coal area} \\ m \cdot n = 0.91 \sim 1.13, \ \textit{Transition area} \\ m \cdot n = 0.98 \sim 1.14, \textit{Up-mining area} \end{cases} \tag{3}$$

## 4. Fracture Structure of Overlying Strata and Mechanism of Strata Pressure Zoning

### *4.1. Establishment of the Numerical Model*

The "trial and error method" [35] was employed for parameter fitting, resulting in the development height of the "two zones" as shown in Figure 10. The development height of the fracture zone is 29 m, and the numerical simulation results are consistent with the measured data of the "two zones" in Section 2.4. This proves that the chosen physical and mechanical parameters in this paper can accurately reflect the rock strata movement characteristics in Yongming Coal Mine. The lithological parameters for each stratum are presented in Table 5.

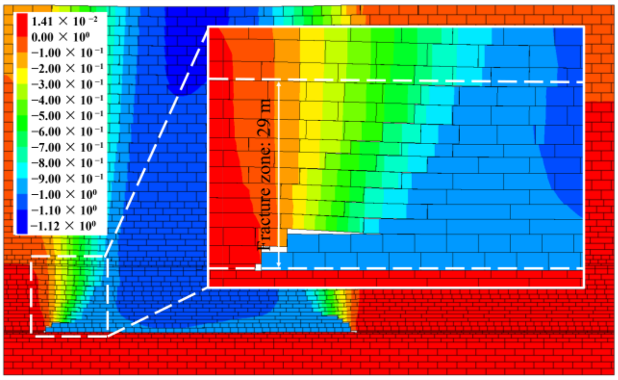


**Figure 10.** Development height of the "two zones".

**Table 5.** Rock strata lithological parameters.

| No. | Lithology | *H*/m | *G*/GPa | *K*/GPa | $\rho$/(g/cm$^3$) | *C*/MPa | $\Phi$/(°) | $R_T$/MPa |
|---|---|---|---|---|---|---|---|---|
| 1 | Loose layer | 120.00 | 0.7 | 0.36 | 1.83 | 3.2 | 28 | 0.10 |
| 2 | Fine sandstone | 16.50 | 1.66 | 1.20 | 2.32 | 1.82 | 35 | 0.98 |
| 3 | Mudstone | 7.00 | 2.40 | 1.01 | 2.22 | 2.48 | 35 | 1.26 |
| 4 | Siltstone | 10.86 | 2.49 | 3.02 | 2.60 | 2.51 | 26 | 1.36 |
| 5 | Mudstone | 5.22 | 2.60 | 1.01 | 2.22 | 2.48 | 35 | 1.26 |
| 6 | Coal seam No. 5 | 1.10 | 0.90 | 0.23 | 1.36 | 0.50 | 28 | 1.03 |
| 7 | Mudstone | 2.00 | 2.40 | 1.01 | 2.22 | 2.48 | 35 | 1.26 |
| 8 | Siltstone | 6.90 | 2.49 | 1.03 | 2.60 | 2.51 | 26 | 1.36 |
| 9 | Fine sandstone | 10.80 | 1.66 | 1.20 | 2.32 | 1.82 | 35 | 0.98 |
| 10 | Mudstone | 6.00 | 2.40 | 1.01 | 2.22 | 2.48 | 35 | 1.26 |
| 11 | Siltstone | 6.30 | 2.49 | 1.06 | 2.60 | 2.51 | 26 | 1.36 |
| 12 | Mudstone | 5.60 | 2.40 | 1.01 | 2.22 | 2.48 | 35 | 1.26 |
| 13 | Coal seam No. 3 | 0.70 | 0.90 | 0.23 | 1.31 | 0.50 | 30 | 1.03 |
| 14 | Mudstone | 1.60 | 2.40 | 1.01 | 2.22 | 2.48 | 35 | 1.26 |
| 15 | Siltstone | 4.90 | 2.49 | 1.06 | 2.60 | 2.51 | 26 | 1.36 |
| 16 | Fine sandstone | 20.00 | 1.66 | 1.20 | 2.32 | 1.82 | 35 | 0.98 |

According to Figures 1b and 2a, the 3105 mining face and the 1515 mining face are chosen for simulation excavation using Universal Distinct Element Code 7.0 (UDEC 7.0) software. The lengths of the 3105 and 1515 mining faces are both 200 m, with 20 m and 50 m coal pillars reserved on the left side of the 3105 mining face and the right side of the 1515 mining face, respectively. The model was constructed upwards from the floor of the 3105 mining face along the fine sandstone strata, reaching the ground. The strata were divided into 16 layers, resulting in a model size of length × width = 380 m × 228 m. Since the dip angle of the coal seam is 1~3°, it is considered a horizontal coal seam. The left and right sides of the model limit the level, the bottom limits the vertical displacement, and the top is a free boundary. The model is calculated using the Mohr–Coulomb criterion, and support units are used to simulate hydraulic support. The numerical model is illustrated in Figure 11. After the initial equilibrium of the model, the 3105 mining face will be excavated first according to the actual mining sequence. Once the 3105 mining face excavation has stabilized, the 1515 mining face will be excavated. Simultaneously with the excavation of the 1515 mining face, hydraulic supports are installed, and a survey line is arranged on the roof of the 1515 mining face, divided into 12 sections with a total of 13 points. The vertical stresses of these points are recorded as the load for the hydraulic supports 10#, 20#, 30#, 40#, 50#, 60#, 70#, 80#, 90#, 100#, 110#, 120#, and 130#. Notably, the 72# support is positioned directly above the right boundary of the 3105 mining face.

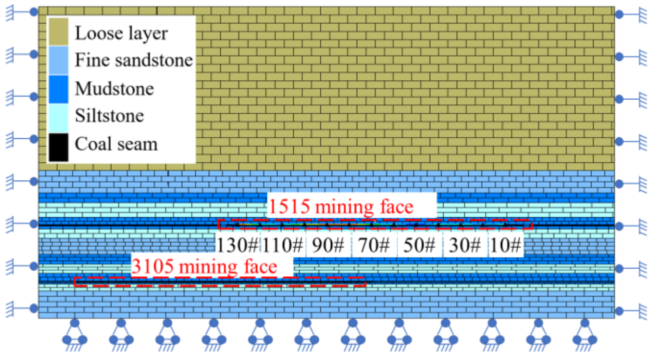


**Figure 11.** Numerical model.

*4.2. Characteristics of Overlying Strata after Excavation of Lower Coal Seam*

Based on the numerical model, the characteristics of the overlying strata after the excavation of the lower coal seam are studied. The structural features of the overlying strata after the excavation of the 3105 mining face are analyzed. After the excavation of the lower coal seam, the rock structure is closely related to stress. The 1515 mining face is analyzed based on the characteristics and stress distribution of the overlying strata. Figure 12 shows the zoning characteristics and vertical stress distribution of the overlying strata after the excavation of the lower coal seam.

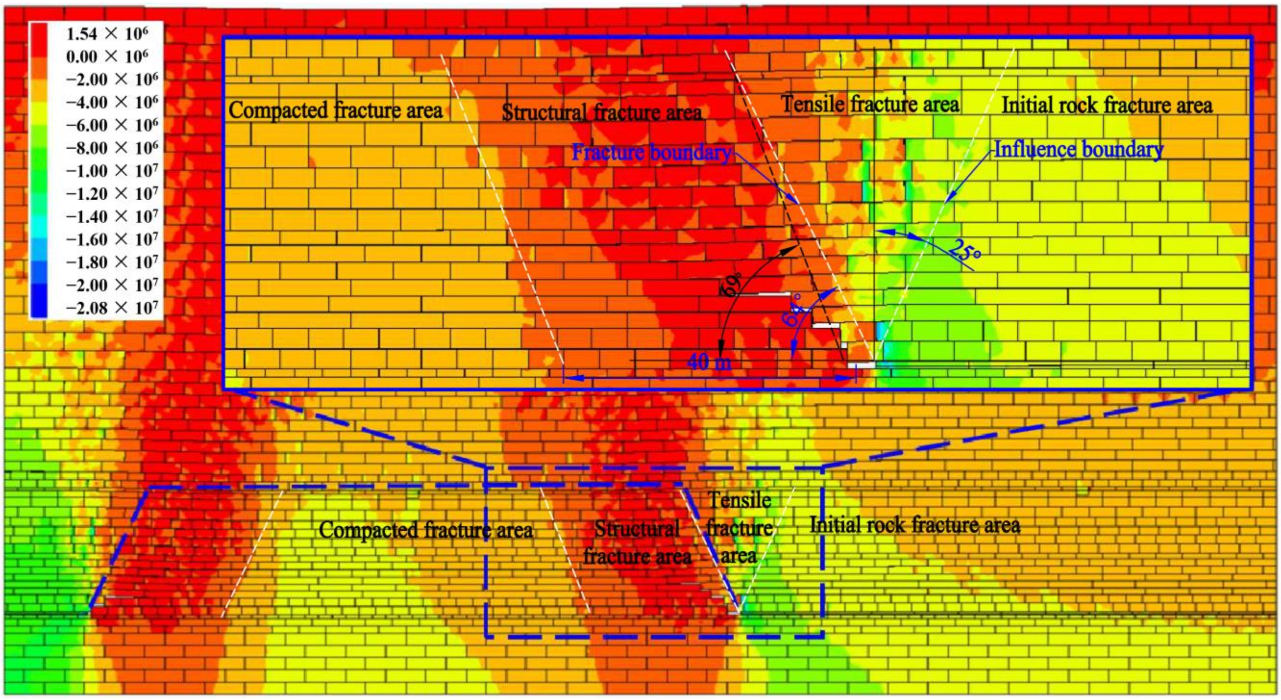


**Figure 12.** Overlying strata zoning characteristics and stress distribution map after excavation of the lower coal seam.

As shown in Figure 12, the immediate roof of the 3105 mining face in the lower coal seam completely caves after excavation. The breaking angle is 64°, the displacement angle is 25°, and the length of the structural fracture area is 40 m. The measured results are generally consistent with the theoretical calculation results in Table 4.

The rock outside the influence boundary is minimally affected by the mining of the 3105 mining face and maintained its initial rock stress state, belonging to the initial rock fracture area. In the area located between the influence boundary and the fracture boundary, some rock strata are above the coal pillar, while others are above the goaf, forming a structure resembling a "cantilever beam". This results in a large number of vertical fractures in the rock strata, indicative of a tensile fracture area. Although the main roof adjacent to the tensile fracture area experiences fractures, the rock blocks of the main roof are hinged due to the horizontal thrust generated during the rotation, forming a "masonry beam" structure. The abutment pressure in this area is low, representing a structural fracture area, with a range of approximately 40 m. Adjacent to the structural fracture area is the compacted fracture area, where vertical stress gradually increased, causing the separation and fractures to close again and compact.

### *4.3. Load Distribution Law for Hydraulic Support in Upper Mining Face*

As shown in Figure 13, the hydraulic support load exhibits a clear non-uniform distribution characteristic, and its distribution trend matches the measured results shown in Figure 6b. After dividing into the "horizontal four areas" as shown in Figure 13, it is observed that supports 10# to 59# are located in the initial rock fracture area. The support load from the goaf boundary to the center of the goaf exhibits a characteristic distribution of first rising, then falling, and then rising again. Supports 60# to 84# are located in the tensile fracture area, and the overall support load showed a downward trend. The load of support 60# reaches the maximum load value for the entire mining face. Supports 85# to 110# are located in the structural fracture area. Although the support load in this area fluctuates slightly, it is smaller than the initial rock fracture area and tensile fracture area overall. Supports 111# to 130# are located in the compacted fracture area, and the support load first rose and then fell, similar to the load distribution trend of supports 10# to 30# in the initial rock fracture area.

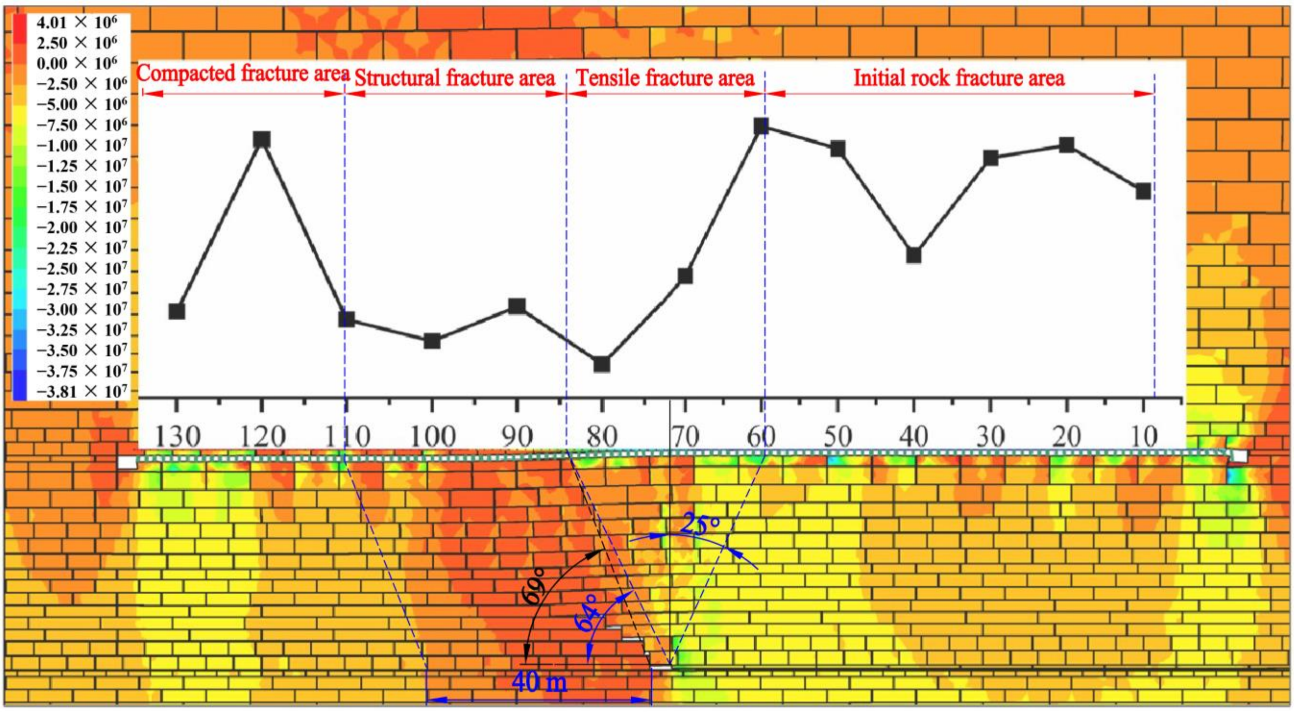


**Figure 13.** Hydraulic support load diagram.

### *4.4. Load Checking Calculation for Hydraulic Support Based on Zoning Characteristics of Overlying Strata Structure*

This section further investigated the intrinsic relationship between the load on the hydraulic supports in the upward mining face across half of the goaf along the panel direction and the height of the roof separation, as well as the length of the hanging roof. Combining the theoretical analysis results of the zoning separation height and the hanging roof length from Section 3.2, simulations of support loads for both the entity coal area and the up-mining area were carried out. A survey line was arranged above the hydraulic supports to monitor the support load. The average vertical stress at each point on the survey line was taken as the hydraulic support loads. The results are shown in Figure 14. The hydraulic support load in the up-mining area is 28.1 MPa, while in the entity coal area, it is 27.2 MPa. The ratio of support load in the up-mining area to that in the entity coal area is 1.03, which aligns well with the theoretical calculation of hydraulic support load in Section 3.2 (0.98~1.14). This indicates that the height of the immediate roof separation and the length of the hanging roof are the main factors affecting the hydraulic support load distribution. The results also reveal that the mining face in the up-mining area has a high height for the immediate roof separation and a short hanging roof length. The mining face in the entity coal area has a low height for the immediate roof separation and a long hanging roof length.

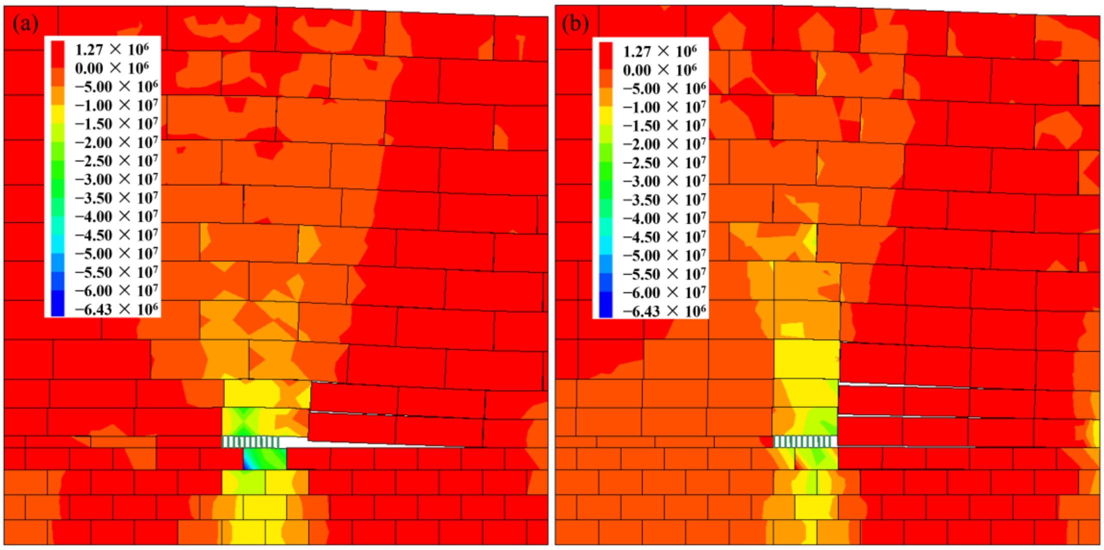


**Figure 14.** Development characteristics of the roof in the upper mining face: (**a**) support load in the entity coal area; (**b**) support load in the up-mining area.

## 5. Conclusions

The measured maximum height of the overlying strata fracture zone in the lower coal seam mining face was 29.58 m, indicating that the 1515 upward mining face across half of the goaf along the panel direction was situated in a curved subsidence zone. Through a combination of field measurements, theoretical analysis, and numerical simulations, the overlying strata structure and the mechanism of strata pressure zoning in the 1515 upward mining face across half of the goaf along the panel direction were investigated, and the conclusions are as follows.

1. The support load in the upward mining face across half of the goaf along the panel direction exhibited distinct zoning characteristics. The hydraulic support loads in the 1515 upward mining face followed a pattern of alternating low- and high-pressure distributions from the up-mining area to the entity coal area. The maximum support load was 1.37 times the minimum support load. This indicated that the upward mining face in the curved subsidence zone is still influenced by the fracture structure zoning of the overlying strata in the lower coal seam.
2. The variations in the overlying strata fracture structure in the upward mining face across half of the goaf along the panel direction were the underlying reasons for differences in the distribution pattern of the mine pressure. Different regions exhibited significantly different heights of the immediate roof development. The development height of the immediate roof separation in the compacted fracture area was 1.74 times that of the entity coal area, at 9.1 m and 5.22 m, respectively. Compared to the initial

rock fracture area, the hanging roof length in the tensile fracture area and structural fracture area was shorter, and the separation height was greater. In the compacted fracture area, the hanging roof length was the smallest, while the separation height was the largest. These factors were the primary influences on the support load zoning.

3. Based on the structural characteristics of overlying strata fractures in different zoning, the immediate roof height variation coefficient ($m$) and the hanging roof coefficient ($n$) were introduced. A zoning and calculation method for the support load in the upward mining face across half the goaf along the panel direction was proposed. The study provided ranges for key parameters related to the support load in each zoning. Numerical simulations yielded a ratio of support load in the up-mining area to the entity coal area of 1.03, demonstrating a good correspondence with the zoning calculation method for the hydraulic support load.

**Author Contributions:** Conceptualization, Y.Z. and F.M.; methodology, Y.Z. and S.Z.; software, F.M. and S.Z.; validation, Y.Z. and S.Z.; investigation, F.M., Q.W., X.Z., S.L. and Y.C.; resources, G.F.; writing—original draft preparation, F.M.; writing—review and editing, Y.Z. and S.Z.; project administration, J.L., G.F. and S.Z.; funding acquisition, Y.Z., G.F. and S.Z. All authors have read and agreed to the published version of the manuscript.

**Funding:** This research was funded by the National Natural Science Foundation of China, grant numbers 52374100, 52304150 and 52004172; Distinguished Youth Funds of National Natural Science Foundation of China, grant number 51925402; China Postdoctoral Science Foundation-funded project, grant number 2020M682215; Fundamental Research Program of Shanxi Province, grant number 202203021212252.

**Data Availability Statement:** The data presented in this study are available on request from the corresponding author.

**Conflicts of Interest:** Author Jie Li was employed by the company Shaanxi Yongming Coal Mine Co., Ltd. Author Yujiang Zhang is part of Postdoctoral Centre in Shandong Energy Group Co., Ltd. The remaining authors declare that the research was conducted in the absence of any commercial or financial relationships that could be construed as a potential conflict of interest.

## References

1. Liu, H.; Zuo, J.; Zhang, C.; Kaijun, W.; Lei, B. Asymmetric deformation mechanism and control technology of roadway under room-pillar group in huasheng coal mine. *J. Cent. South Univ.* **2023**, *30*, 2284–2301. [CrossRef]
2. Hu, R.; Wu, J.; Shi, W.; Zhai, X.; Huang, K. Study on Evolution Characteristics of Regenerated Roof Structure in Downward Mining of Bifurcated Coal Seam. *Adv. Mater. Sci. Eng.* **2021**, *2021*, 8226616. [CrossRef]
3. Hu, R.; Wu, J.; Zhai, X.; Shi, W.; Huang, K. Structural characteristics of regenerated roof and distribution law of overburden porosity in downward mining of a bifurcated coal seam. *Geofluids* **2022**, *2022*, 6914746. [CrossRef]
4. Yang, K.; Fu, Q.; Liu, Q.; He, X.; Lyu, X. Evolution of Mining-Induced Stress in Downward Mining of Short-Distance Multiseam. *Geofluids* **2022**, *2022*, 3305734. [CrossRef]
5. Tang, L.; Liang, S. Study on the Feasibility of the Upward Mining Above the Goaf of the Irregular Roadway Mining Under the Influence of Hard and Thick Strata. *Geotech. Geol. Eng.* **2019**, *37*, 5035–5043. [CrossRef]
6. Chai, J.; Han, Z.; Lv, W.; Zhu, H.; Hou, S. Research on reasonable layout parameters of working faces based on the concept of harmonic extraction to reduce the damage of coal seam waiting for upward mining. *Sci. Rep.* **2023**, *13*, 21789. [CrossRef]
7. Wu, X.; Wang, S.; Gao, E.; Chang, L.; Ji, C.; Ma, S.; Li, T. Failure mechanism and stability control of surrounding rock in mining roadway with gentle slope and close distance. *Eng. Fail. Anal.* **2023**, *152*, 107489. [CrossRef]
8. Liu, R. Research and Application of Roadway Support Technology for Upward Mining of Protected Seam in Close Distance Coal Seam. Master's Thesis, Anhui University of Science and Technology, Huainan, China, 2022.
9. Bian, W.; Yang, J.; He, M.; Zhu, C.; Xu, D. Research and application of mechanical models for the whole process of 110 mining method roof structural movement. *J. Cent. South Univ.* **2022**, *29*, 3106–3124. [CrossRef]
10. Feng, G. Study on the Theory and Its Application of Upward Mining of Left-Over Coal. Ph.D. Thesis, Taiyuan University of Technology, Taiyuan, China, 2011.
11. Feng, G.; Yan, X.; Wang, X.; Kang, L.; Zhai, Y. Determination of key positions of strata controlling in rocks between coal seams for upward mining. *Chin. J. Rock Mech. Eng.* **2009**, *28*, 3721–3726.
12. Feng, G.; Yan, Y.; Yang, S.; Zhang, B.; Zhai, Y.; Kang, L. Analysis on the damage zone of overlying strata and safety layer distanceon the upward mining above the longwall goaf. *J. China Coal Soc.* **2009**, *34*, 1032–1036.

13. Ma, L.; Wang, L.; Qiao, J.; Wang, S. Study of ascending mining of short-range-seams in pingdingshan no.4 coal mine. *J. Min. Saf. Eng.* **2008**, *25*, 357–360.
14. Zhang, H.; Han, J.; Hai, L.; Li, M.; Qiao, H. Study on closed multiple-seam in the ascending mining technology. *J. Min. Saf. Eng.* **2013**, *30*, 63–67.
15. Zhang, C. Study on overlying strata caving and movement regularity of ascending mining in contiguous seams. *Coal Sci. Technol.* **2018**, *46*, 1–7. [CrossRef]
16. Kong, D.; Pu, S.; Zheng, S.; Wang, C.; Lou, Y. Roof Broken Characteristics and Overburden Migration Law of Upper Seam in Upward Mining of Close Seam Group. *Geotech. Geol. Eng.* **2019**, *37*, 3193–3203. [CrossRef]
17. Wang, Y.; Fu, X.; Kong, L.; Zhao, Y.; Zhang, N. Study on stability of dangling structure in ascending mining contiguous coal seams. *Coal Sci. Technol.* **2020**, *48*, 95–100. [CrossRef]
18. Peng, S. *Coal Mine Ground Control*, 1st ed.; John Wiley & Sons Inc.: Hoboken, NJ, USA, 1978; pp. 37–44.
19. Qian, M.; Shi, P.; Xu, J. *Rock Pressure and Strata Control*, 2nd ed.; Publishing House of China University of Mining and Technology: Xuzhou, China, 2010; pp. 73–99.
20. Liu, T. The possibility of using the upward mining method. *J. China Coal Soc.* **1981**, *1*, 18–29.
21. Wang, L. The Technology and Application of Ascending Mining in Coal Seams. In *Academic Symposium on High Efficiency and Intensive Mine in the 21st Century, Beijing, China*; Editorial Department of Journal of China Coal Society: Beijing, China, 2001; p. 4.
22. Guo, M.; Guo, W.; Yuan, R.; Zhao, G.; Bai, E.; Li, G. Spatial Location Determination Of Directional Boreholes Based On Regional Distribution Characteristics Of Mining-Induced Overburden Fractures. *J. Min. Saf. Eng.* **2022**, *39*, 817–826. [CrossRef]
23. Wu, F.; Yue, X.; Liu, C.; Yu, C.; Liu, Q.; Li, C.; Du, B.; Yang, P.; Chen, Y. Movement law of overburden in steep inclined ultra thick seam and calculation of support working resistance. *J. Min. Saf. Eng.* **2022**, *39*, 499–506. [CrossRef]
24. Li, Y.; Ren, Y.; Li, T.; Yang, K.; Jin, X. Calculation and system of support resistance of shield for contugous-multiple coal seams with coordinated mining. *Coal Sci. Technol.* **2023**, *51*, 268–277. [CrossRef]
25. Singh, G.; Singh, U. Prediction of caving behavior of strata and optimum rating of hydraulic powered support for longwall workings. *Int. J. Rock Mech. Min. Sci.* **2010**, *47*, 1–16. [CrossRef]
26. Juárez-Ferreras, R.; González-Nicieza, C.; Menéndez-Díaz, A.; Álvarez-Vigil, A.E.; Álvarez-Fernández, M.I. Measurement and analysis of the roof pressure on hydraulic props in longwall. *Int. J. Coal Geol.* **2008**, *75*, 49–62. [CrossRef]
27. Ma, L.; Wang, L.; Zhang, D.; Liu, Y.; Liu, J.; Zhang, T.; Ouyang, G. Application and study on feasibility of near distance coal seam group ascending mining. *J. Hunan Univ. Sci. Technol.* **2007**, *22*, 1–5.
28. Zhang, Y.; Wang, Y.; Cui, B.; Feng, G.; Zhang, S.; Zhang, C.; Zhang, Z. A disturbed voussoir beam structure mechanical model and its application in feasibility determination of upward mining. *Energies* **2023**, *16*, 7190. [CrossRef]
29. Xu, Y. *Coal Mining Science*, 1st ed.; China University of Mining and Technology Pres: Xuzhou, China, 2015; p. 211.
30. Liu, Z.; Zhang, S.; Huangfu, L. Overburden Migration Law of Inclined Coal Seam and Determination of "Upper Three Zones" Height in Tengda Coal Mine. *J. Min. Strat. Control Eng.* **2022**, *4*, 70–79. [CrossRef]
31. Liu, Y.; Cheng, J.; Jiao, J.; Meng, X. Feasibility study on multi-seam upward mining of multi-layer soft-hard alternate complex roof. *Environ. Earth Sci.* **2022**, *81*, 424. [CrossRef]
32. Marinina, O.; Nechitailo, A.; Stroykov, G.; Tsvetkova, A.; Reshneva, E.; Turovskaya, L. Technical and economic assessment of energy efficiency of electrification of hydrocarbon production facilities in underdeveloped areas. *Sustainability* **2023**, *15*, 9614. [CrossRef]
33. Zhang, Y.; Cui, B.; Wang, Y.; Zhang, S.; Feng, G.; Zhang, Z. Evolution Law of Shallow Water in Multi-Face Mining Based on Partition Characteristics of Catastrophe Theory. *Fractal Fract.* **2023**, *7*, 779. [CrossRef]
34. Shen, H. Research on Feasibility of Upward Ming and Reasonablelocation of Roadway in Yongning Coal Mine. Master's Thesis, Taiyuan University of Technology, Taiyuan, China, 2019.
35. Liu, Y.; Wu, Z.; Chu, Z.; Weng, L.; Xu, X.; Zhou, Y.; Gao, B.; Mao, C. Rock breaking mechanism with mechanical impact under confining pressure based on FDEM. *J. Cent. South Univ. (Sci. Technol.)* **2023**, *54*, 866–879. [CrossRef]


**Disclaimer/Publisher's Note:** The statements, opinions and data contained in all publications are solely those of the individual author(s) and contributor(s) and not of MDPI and/or the editor(s). MDPI and/or the editor(s) disclaim responsibility for any injury to people or property resulting from any ideas, methods, instructions or products referred to in the content.